

University of Groningen

## A High Cell-Bearing Capacity Multibore Hollow Fiber Device for Macroencapsulation of Islets of Langerhans

Skrzypek, Katarzyna; Groot Nibbelink, Milou; Liefers-Visser, Jolanda; Smink, Alexandra M; Stoimenou, Eleftheria; Engelse, Marten A; de Koning, Eelco J P; Karperien, Marcel; de Vos, Paul; van Apeldoorn, Aart

*Published in:*  
Macromolecular Bioscience

*DOI:*  
[10.1002/mabi.202000021](https://doi.org/10.1002/mabi.202000021)

**IMPORTANT NOTE: You are advised to consult the publisher's version (publisher's PDF) if you wish to cite from it. Please check the document version below.**

*Document Version*  
Publisher's PDF, also known as Version of record

*Publication date:*  
2020

[Link to publication in University of Groningen/UMCG research database](#)

### *Citation for published version (APA):*

Skrzypek, K., Groot Nibbelink, M., Liefers-Visser, J., Smink, A. M., Stoimenou, E., Engelse, M. A., de Koning, E. J. P., Karperien, M., de Vos, P., van Apeldoorn, A., & Stamatialis, D. (2020). A High Cell-Bearing Capacity Multibore Hollow Fiber Device for Macroencapsulation of Islets of Langerhans. *Macromolecular Bioscience*, 20(8), [2000021]. <https://doi.org/10.1002/mabi.202000021>

### **Copyright**

Other than for strictly personal use, it is not permitted to download or to forward/distribute the text or part of it without the consent of the author(s) and/or copyright holder(s), unless the work is under an open content license (like Creative Commons).

The publication may also be distributed here under the terms of Article 25fa of the Dutch Copyright Act, indicated by the "Taverne" license. More information can be found on the University of Groningen website: <https://www.rug.nl/library/open-access/self-archiving-pure/taverne-amendment>.

### **Take-down policy**

If you believe that this document breaches copyright please contact us providing details, and we will remove access to the work immediately and investigate your claim.



# A High Cell-Bearing Capacity Multibore Hollow Fiber Device for Macroencapsulation of Islets of Langerhans

Katarzyna Skrzypek, Milou Groot Nibbelink, Jolanda Liefers-Visser, Alexandra M. Smink, Eleftheria Stoimenou, Marten A. Engelse, Eelco J. P. de Koning, Marcel Karperien, Paul de Vos, Aart van Apeldoorn, and Dimitrios Stamatialis\*


Macroencapsulation of islets of Langerhans is a promising strategy for transplantation of insulin-producing cells in the absence of immunosuppression to treat type 1 diabetes. Hollow fiber membranes are of interest there because they offer a large surface-to-volume ratio and can potentially be retrieved or refilled. However, current available fibers have limitations in exchange of nutrients, oxygen, and delivery of insulin potentially impacting graft survival. Here, multibore hollow fibers for islets encapsulation are designed and tested. They consist of seven bores and are prepared using nondegradable polymers with high mechanical stability and low cell adhesion properties. Human islets encapsulated there have a glucose induced insulin response (GIIS) similar to nonencapsulated islets. During 7 d of cell culture in vitro, the GIIS increases with graded doses of islets demonstrating the suitability of the microenvironment for islet survival. Moreover, first implantation studies in mice demonstrate device material biocompatibility with minimal tissue responses. Besides, formation of new blood vessels close to the implanted device is observed, an important requirement for maintaining islet viability and fast exchange of glucose and insulin. The results indicate that the developed fibers have high islet bearing capacity and can potentially be applied for a clinically applicable bioartificial pancreas.

## 1. Introduction

Clinical islet transplantation (CIT) in the liver via the infusion of islets into the portal vein has been explored as a potential therapy for patients with type 1 diabetes.<sup>[1]</sup> However, CIT is associated with a high degree of islet loss due to their exposure to several stress factors within the first two weeks after intervention.<sup>[2]</sup> In addition, this is only applied in a small group of severe diabetic patients as immunosuppression has to be applied to prevent graft rejection which as such has severe side effects. Extrahepatic islet transplantation using biomaterials as an immunoprotective islet carrier could improve the outcome of the transplantation by providing a more optimal environment and potentially allow for transplantation in the absence of immunosuppression.<sup>[3]</sup> In fact, the encapsulation of pancreatic islets, or beta cells, within semipermeable membranes represents a promising strategy to immobilize transplanted islets in one location outside

Dr. K. Skrzypek, Prof. D. Stamatialis  
Bioartificial Organs  
Biomaterials Science and Technology Department  
Faculty of Science and Technology  
TechMed Centre  
University of Twente  
Enschede 7500AE, The Netherlands  
E-mail: d.stamatialis@utwente.nl

Dr. M. Groot Nibbelink, Prof. M. Karperien  
Developmental BioEngineering  
Faculty of Science and Technology  
TechMed Centre  
University of Twente  
Enschede 7500AE, The Netherlands

 The ORCID identification number(s) for the author(s) of this article can be found under <https://doi.org/10.1002/mabi.202000021>.

© 2020 The Authors. Published by WILEY-VCH Verlag GmbH & Co. KGaA, Weinheim. This is an open access article under the terms of the Creative Commons Attribution License, which permits use, distribution and reproduction in any medium, provided the original work is properly cited.

DOI: 10.1002/mabi.202000021

Dr. J. Liefers-Visser, Dr. A. M. Smink, Prof. P. de Vos  
Pathology and Medical Biology  
Section Immunoendocrinology  
University of Groningen  
University Medical Center Groningen  
Groningen 9713GZ, The Netherlands

E. Stoimenou  
Faculty of Sciences, School of Biology  
Aristotle University of Thessaloniki  
Thessaloniki 54124, Greece

Dr. M. A. Engelse, Prof. E. J. P. de Koning  
Nephrology  
Leiden University Medical Center  
Leiden 2333ZA, The Netherlands

Prof. E. J. P. de Koning  
Hubrecht Institute  
Utrecht 3584CT, The Netherlands

Dr. A. van Apeldoorn  
Complex Tissue Regeneration  
MERLN Institute for Technology Inspired Regenerative Medicine  
Maastricht University  
Maastricht 6229ER, The Netherlands

the liver and provide optimal spatial and functional support, which could ultimately lead to enhanced islet survival.<sup>[4]</sup> Intravascular systems often require a complex surgical intervention with varying successful outcome, while extravascular systems have the great advantage of relatively easy implantation and potential retrieval. Additionally, extravascular devices can be reloaded and replaced when necessary.<sup>[4b,5]</sup> This latter is a pertinent consideration since emerging new replenishable cell sources become available, such as insulin producing cells obtained from stem-cells, which still have functional limitations requiring retrievability.<sup>[6]</sup>

An important challenge in creating an optimal microdevice is to create a device with proper transport properties of nutrients and oxygen to the islets and, at the same time, protect the encapsulated islets from the host-immune system.<sup>[5,7]</sup> The configurations proposed for a membrane-based macroencapsulation device include flat and hollow fiber membranes.<sup>[4b]</sup> In comparison to the flat membranes, the hollow fibers are quite attractive, offering a combination of high surface area with a compact design, which is desirable for implantable devices.<sup>[8]</sup> In addition to this, to guarantee survival of the encapsulated cells in the fiber, several parameters need to be taken into consideration. The inside membrane material should preferably have low cell adhesive properties to avoid islet attachment onto the inner membrane surface, which could lead to loss of phenotype and subsequently their endocrine function.<sup>[9]</sup> Additionally, the fiber diameter should be designed to tightly fit pancreatic islets, while the wall thickness should be low and the membrane porosity high to decrease the diffusion distance and provide optimal mass transport.<sup>[4b]</sup>

Improvements in hollow fibers for renal dialysis also stimulated application of these fibers for cell encapsulation including intra- and extravascular macrodevices.<sup>[4b]</sup> The newer generation fibers have thin walls to achieve optimal mass transport. However, when applied for islet encapsulation, they often suffered from insufficient material biocompatibility or mechanical instability. Additionally, due to their dimensions, the oxygen and nutrients diffusion was limited and occlusion of fibers could occur contributing to diffusion issues and shorter graft survival times.<sup>[10]</sup> Another important issue for the single fibers was the need for accommodating a high number of islets to be able to restore normoglycemia.<sup>[1b]</sup> A modeling study of Dulong and Legallais has shown how challenging the fiber optimization is to achieve sufficient loading of islets to induce normoglycemia.<sup>[11]</sup> In order to increase the total amount of islets in single bore hollow fiber devices, the length of the fibers needs to be increased to lengths that make their clinical application unrealistic.<sup>[12]</sup>

Here, we designed and tested a novel fiber-based system in which aforementioned challenges have been taken into account. To this end a novel multibore system was engineered for islet encapsulation. In comparison to a conventional single bore fiber, the multibore fiber offers more space for islet encapsulation within the same fiber length and without significant increase in volume of the device. Additionally, multibore configuration has been shown to improve mechanical stability and handling of the fibers<sup>[13]</sup> which are important considerations during implantation. The multibore fibers with small

bore diameter (500  $\mu\text{m}$ ) is tailored to fit the broad size range of pancreatic islets (50–350  $\mu\text{m}$ ). Nondegradable polyethersulfone (PES) is used as a membrane forming material, blended with the hydrophilic additive polyvinyl-pyrrolidone (PVP). The PES/PVP blend is used for hemodialysis membrane fabrication and does not allow significant inflammatory cell adhesion which is very important for biocompatibility.<sup>[14]</sup> The characteristics of the new multibore fibers are tailored to achieve efficient nutrient delivery to the cells and insulin delivery to the surrounding vessels by the encapsulated insulin producing cells. In fact, the walls of the bores are fabricated as thin as possible without compromising membrane stability. As a proof of concept, the multibore hollow fibers are evaluated by analyzing the glucose-induced insulin responsive human cadaveric islets encapsulated in the device. Nonencapsulated, free floating islets are used as control. Our results are compared to those obtained for islets encapsulated into commercially available multibore fibers with large bore diameter (900  $\mu\text{m}$ ), previously used as hepatocyte bioreactors and 3D tissue engineering applications.<sup>[15]</sup> Moreover, the multibore fiber material biocompatibility and the formation of new blood vessels around the fiber are assessed after subcutaneous implantation in mice, as a first step toward clinical assessment of the device.

## 2. Experimental Section

### 2.1. Multibore Hollow Fiber Fabrication

The multibore hollow fibers were fabricated by dry-wet spinning via immersion precipitation using a specially designed spinneret (Figure S1A, Supporting Information). The polymer dope solution was a blend of 15 wt% PES (Ultron E6020) and 10 wt% polyvinylpyrrolidone (PVP K90, Sigma Aldrich) dissolved in N-methylpyrrolidone (NMP) (Acros organic). After 24 h mixing on a roller bank, the solution was filtered using a 15  $\mu\text{m}$  filter (Bekipor ST AL3, Bekaert) into a stainless-steel syringe and left to degas overnight. The following day, the syringe and the bore solution were mounted in the high-pressure syringe pumps and connected to a specially designed spinneret (Figure S1B, Supporting Information). Subsequently, the spinneret was placed above the coagulation bath at a fixed height (air gap). The polymer dope and bore solution were pumped through the spinneret and after a 6 cm air gap, the nascent multibore hollow fiber was immersed into the water coagulation bath, where phase separation occurred, and the fiber was formed. The multibore hollow fibers were collected in a free-falling way. During spinning, several parameters were varied, which are described in **Table 1**. The collected hollow fiber membranes were washed with demineralized water in order to remove remaining solvent traces and stored in demineralized water until further use.

To increase the membrane porosity, the PVP of some of the developed fibers was washed with 4000 ppm sodium hypochlorite aqueous solution (NaClO, Fluka) for 24 h. Subsequently, the membranes were washed and stored in demineralized water. Prior to drying, the membranes were immersed in a 25 vol% glycerol solution for 24 h to protect the hollow fiber structure and morphology during air drying.

**Table 1.** Spinning conditions.

Multibore hollow fiber	MF1	MF2	MF3
Polymer dope	15 wt% PES 10 wt% PVP	15 wt% PES 10 wt% PVP	15 wt% PES 10 wt% PVP
Bore liquid	Water	50% NMP in water	50% NMP in water
Coagulation bath	Water	Water	Water
Coagulation bath temperature	19–21 °C	19–21 °C	48–50 °C
Polymer dope pumping speed [mL min <sup>-1</sup> ]	1.0	1.0	1.0
Bore liquid pumping speed [mL min <sup>-1</sup> ]	4.3	4.3	4.3
Air gap [cm]	6.0	6.0	6.0

## 2.2. Scanning Electron Microscopy

The multibore hollow fiber membrane morphology was visualized using scanning electron microscopy (SEM, JEOL JSM-IT 100). The membranes were dried in air followed by fracturing in liquid nitrogen to reveal the cross section. Subsequently, samples were clamped in a cross-section holder and sputter-coated with 2 nm-thick gold layers prior to imaging.

## 2.3. Water Transport through the Membrane

Multibore hollow fibers were dried in air and modules were prepared by putting the fiber inside the 10 cm long tube with a Kartell T-connection (VWR) in the middle. Both ends were glued using two-component epoxy glue (Griffon) and cut open after the glue had hardened, opening the bores of the multibore hollow fiber. Before testing, the modules were washed with ultrapure water and prepressurized at 0.7 bar for 1 h, then transmembrane pressures of 0.7, 0.5, and 0.3 bar were applied, and the flux of the permeated ultrapure water was measured over time (in L m<sup>-2</sup> h<sup>-1</sup>). The clean water permeability (L<sub>p</sub>, in L m<sup>-2</sup> h<sup>-1</sup> bar<sup>-1</sup>) was measured in a dead-end mode and determined by calculating the slope of a linear fit of the flux versus transmembrane pressure graph.

## 2.4. Cell Culture

Human islets of Langerhans isolated from four donor pancreata (purity 98%, 95%, 85%, and 75%, respectively) were provided by the Human Islet Isolation Laboratory at the Leiden University Medical Center (Leiden, The Netherlands). Studies were only performed on islets that could not be used for clinical transplantation and after informed consent by the donors. All procedures were carried out in accordance with Dutch law and the relevant guidelines and regulations. The islets were cultured in CMRL 1066 medium (5.5 mmol L<sup>-1</sup> glucose) containing 10% FBS, 2 × 10<sup>-3</sup> M GlutaMAX, 100 U mL<sup>-1</sup> penicillin and 100 µg mL<sup>-1</sup> streptomycin (Gibco), 10 mmol L<sup>-1</sup> HEPES, and 1.2 mg mL<sup>-1</sup> nicotinamide. In order to determine islet

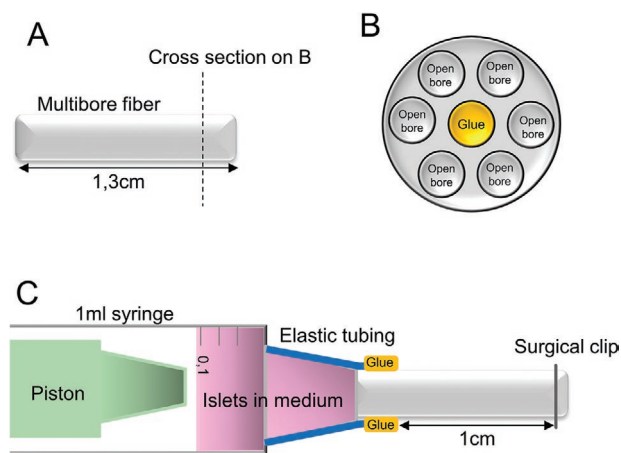


**Figure 1.** Schematic representation of seeding procedure: A) 1.3 cm long multibore hollow fiber, B) cross section of the multibore hollow fiber, where middle bore is closed with the glue and side bores left open, C) fiber is placed in the outlet of the 1 mL syringe and fixed with elastic tubing and the glue and the end of the fiber is closed using surgical clip, islets resuspended in 100 µL of medium are injected inside the open bores.

number, the islets were stained with dithizone (DTZ, 100 µL DTZ per 100 µL islet suspension) and red-stained islets were counted twice in triplicate. The islets were divided and placed in ultralow attachment 24-well plates (Corning) to preserve their morphology and avoid aggregation during culture. Culture medium was refreshed every day.

## 2.5. Cell Seeding

Prior to the cell seeding, the multibore hollow fibers were cut into 1.3 cm pieces and the middle bore of the fiber was closed with glue using two-component epoxy glue (Griffon) (Figure 1A,B). The fibers were then carefully placed at the inlet of the 1 mL syringe and fixed with elastic tubing and glue (see Figure 1C). One end of the fiber was closed using sterile, surgical staples (Teleflex Medical, HORIZON, Ligating clips). The syringe with the attached multibore hollow fiber was sterilized with 70% ethanol, washed in PBS, and preincubated in culture medium overnight. The relevant number of human islets (1000, 3000, or 6000) for the experiments was suspended in 100 µL medium and placed inside the syringe held in perpendicular position with the attached hollow fiber pointing downward. The islet suspension was then carefully injected inside the bores of the fiber with minimal pressure applied on the piston. After injection the multibore hollow fiber was closed with a surgical staple near the inlet and cut off from the syringe leaving 1 cm of fiber with encapsulated islets. Afterward, the fiber was placed in 1 mL of medium and cultured for 1 and 7 d. Culture medium was changed every day.

## 2.6. Human Islets Functionality In Vitro

To assess the function of the encapsulated islets, a glucose-induced insulin secretion test (GIIST) was performed after culture under static conditions for 1 and 7 d. Free-floating

islets in a transwell system (MilliPore) ( $n = 3$ ) were used as positive controls. Fibers containing islets and free-floating nonencapsulated islets of the same donor, as controls, were first preincubated in a modified Krebs buffer ( $115 \times 10^{-3}$  M NaCl,  $5 \times 10^{-3}$  M KCl,  $24 \times 10^{-3}$  M NaHCO<sub>3</sub>,  $2.2 \times 10^{-3}$  M CaCl<sub>2</sub>,  $20 \times 10^{-3}$  M HEPES,  $1 \times 10^{-3}$  M MgCl<sub>2</sub>, 2 mg mL<sup>-1</sup> bovine serum albumin, pH 7.4) for 90 min at 37 °C and 5% CO<sub>2</sub>. Subsequently, the samples were then incubated for 1 h in low ( $1.67 \times 10^{-3}$  M), high ( $16.7 \times 10^{-3}$  M), low, and again high and low glucose buffer, with three times 5 min washing in Krebs buffer between each high and low glucose incubation step. Two additional GIIST steps (second high and third low glucose incubation) in total five, instead of the three steps often used in the literature,<sup>19b,16j</sup> were performed to determine if there is delay in islet response. Samples were taken after each incubation step, spun down (300 g for, 3 min) and the supernatant was stored at -20 °C. Samples were analyzed using a human insulin ELISA kit (Mercodia). The functionality of human islets was determined by determining the amount of insulin secreted and displayed as the glucose-induced insulin stimulation index. For the calculation of the stimulation index, the insulin secretion of all samples was normalized to the insulin secreted during the first low glucose incubation ( $1.7 \times 10^{-3}$  M glucose). 150 islets were used as free-floating positive controls, representing the quality of the islets used for encapsulation. Stimulation index of at least two defines a functional response.

## 2.7. Multibore Fiber Biocompatibility Study

All animal experiments were reviewed and approved by the Institutional Animal Care and Use Committee of the University of Groningen (Groningen, the Netherlands) and carried out in concordance with the institute guidelines. Animals were group housed with ad libitum access to food and water. In vivo biocompatibility of new multibore fibers was determined by subcutaneous implantation in 8-week-old immunocompetent male C57BL/6BrdCrHsd-Tyrc mice (Envigo) ( $n = 5$ ). Before implantation multibore fibers (1 cm) were closed on both ends with a small sized surgical ligating clip (Horizon Ligating Clips, Teleflex Medical). Then, they were sterilized in 70% ethanol followed by three additional washing steps with sterile DPBS (Lonza) and stored in sterile Krebs–Ringer–Hepes (KRH; pH 7.4,  $133 \times 10^{-3}$  M NaCl,  $4.69 \times 10^{-3}$  M KCl,  $1.18 \times 10^{-3}$  M KH<sub>2</sub>PO<sub>4</sub>,  $1.18 \times 10^{-3}$  M MgSO<sub>4</sub>·7H<sub>2</sub>O,  $25 \times 10^{-3}$  M HEPES,  $2.52 \times 10^{-3}$  M CaCl<sub>2</sub>·2H<sub>2</sub>O (all obtained from Merck Millipore) buffer until implantation. Mice were anesthetized using 2–3% of isoflurane (Piramel Healthcare, Morpeth, UK) and, after shaving, a small incision was made on the right flank of the animal. Multibore fibers were then implanted into a subcutaneous pocket made using forceps. At day 28 after implantation, multibore fibers and surrounding tissue were dissected from the subcutaneous pocket. After dissection, samples were fixed in 2% paraformaldehyde (Merck Millipore) and processed for paraffin embedding and sectioning. Paraffin embedded multibore fibers were sectioned at 2 μm and subsequently stained with hematoxylin and eosin (Sigma-Aldrich). To determine blood vessel formation sections were additionally stained for CD31 positive cells. Briefly, following heat-induced antigen retrieval, sections were

transferred and washed in PBS + 0.2% Triton X-100 (PBST). Sections were incubated for 30 min at 20 °C with 5% donkey serum (PBST) and incubated overnight at 4 °C with a primary polyclonal goat-anti-mouse CD31 antibody (R&D, AF3628) in a 1:200 dilution (PBS + 1% BSA). After washing with PBST sections were consequently incubated for 45 min at 20 °C with a secondary donkey-anti-goat alkaline phosphatase antibody (Abcam, Ab6886) in a 1:100 dilution (PBS + 1% BSA). Alkaline phosphatase activity was demonstrated by incubating the sections for 10 min with SIGMAFAST Fast Red (Sigma-Aldrich). A short incubation with hematoxylin was used as nucleic counterstain. Sections were digitalized using the NanoZoomer 2.0-HT multislide scanner (Hamamatsu, Japan). The amount of blood vessels and their distance from the device was determined using Aperia ImageScope software (Leica).

## 2.8. Statistical Analysis

The results are presented as the mean ± standard deviation. Statistical analyses were performed using two-tailed analysis of variance (ANOVA) using SPSS Statistics software (version 24, IBM Corporation) to compare the insulin concentration and stimulation indexes upon glucose stimulation for islets from different donors seeded within multibore hollow fiber membranes. Statistical significance was considered at  $p$ -values <0.05.

## 3. Results

### 3.1. Development of New Multibore Hollow Fiber Membranes

Various batches of multibore hollow fibers with seven bores were produced by dry-wet spinning method. The spinning conditions were tuned in order to obtain mechanically stable fibers with thin walls, suitable for pancreatic islet encapsulation.

**Figure 2** shows representative SEM images of the developed fibers with small bores of about 500 μm (Figure 2B–D) in comparison to the commercially available PESM multibore fibers with bores of 900 μm diameter and rather thick membrane walls (Figure 2A). The first batch of produced membranes (MF1, Figure 2B) had round bores and rather thick outer and inner walls (200–275 μm) with asymmetric membrane pore morphology. Besides, thick dense selective layers containing small pores were present on both sides of the fiber, while in the fiber cross section, we can observe the presence of macrovoids.

In order to decrease the fiber wall thickness, we adapted the spinning conditions by applying 50% v/v NMP in water, as a bore solution. The new fibers, MF2 (Figure 2C), had thinner walls, however, all the bores were deformed, and the membrane mechanical stability was much lower in comparison to MF1 fibers. To improve this while having thin walls, we applied during the spinning process a coagulation bath temperature of 48–50 °C which resulted in stable multibore hollow fibers (MF3) with thin walls and rounded bores (Figure 2D). **Figure 3** shows the detailed morphology of the MF3 membrane cross section at higher magnification. The membrane walls between the bores consist of a very thin dense selective layer with



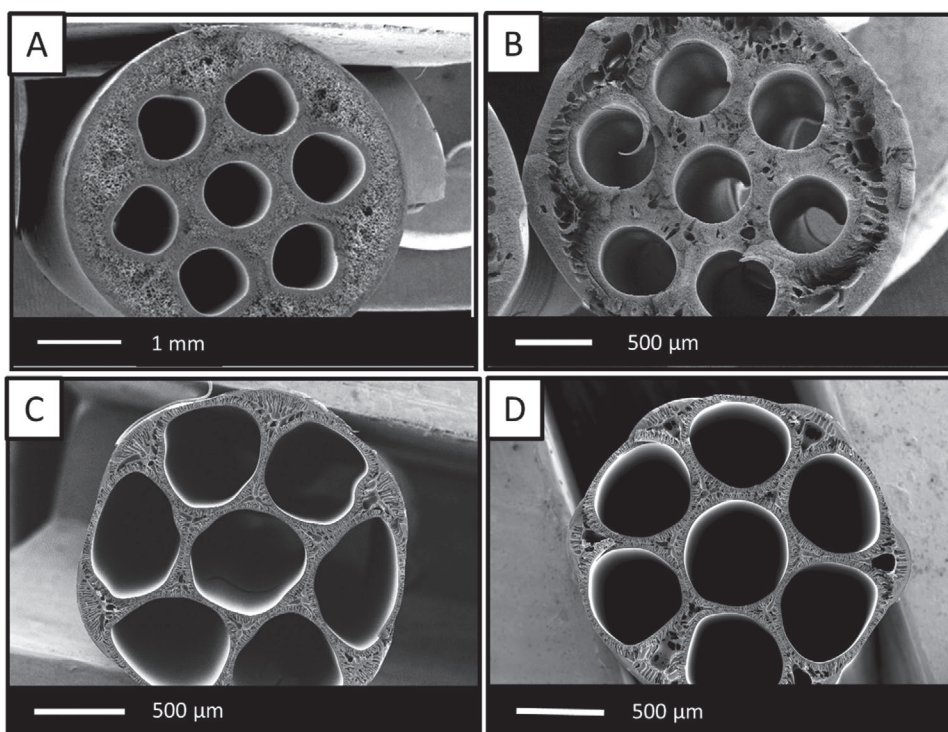


**Figure 2.** Scanning electron microscopy images of multibore hollow fibers: A) Commercial Multibore membrane—PESM, B) MF1, C) MF2, and D) MF3.

small pores, while a finger-like, porous sublayer is present in between. The outer wall of the side bores is around 50  $\mu\text{m}$  thick and less curved resulting in bores slightly flattened on one side. Additionally, the surface of the outer wall of the bores has small pores (1–5  $\mu\text{m}$ ) which are not present at the connections between the bores (Figure 3A). Based on the structural stability and morphology, the MF3 membrane was selected for further characterization and islet encapsulation studies.

### 3.2. Clean Water Transport

Figure 4 presents the clean water flux of the new MF3 multibore membranes at various transmembrane pressures in comparison with commercial multibore hollow fibers. In all cases, the graph is linear indicating good mechanical stability of the membranes in this pressure range. The MF3 membrane has higher water hydraulic permeability (1824  $\text{L m}^{-2} \text{h}^{-1} \text{bar}^{-1}$ ) than the commercial membranes (1023  $\text{L m}^{-2} \text{h}^{-1} \text{bar}^{-1}$ ). Additional treatment with NaClO solution for 24 h, which removes part of the PVP, results in membranes with 40% higher permeability compared to untreated membranes, and more than 100% higher compared to commercial membranes (MF3 washed, 2590  $\text{L m}^{-2} \text{h}^{-1} \text{bar}^{-1}$ ). Therefore, the MF3-washed membranes were chosen as the most suitable for cell encapsulation.

### 3.3. Human Islets Functionality

In order to study the maintenance of endocrine function of islets encapsulated within the multibore hollow fiber, we

performed glucose-induced insulin secretion tests. Figure 5A,B compares the stimulation index of islets encapsulated in the developed fibers in comparison to commercial multibore fibers, PESM, with larger bores and to nonencapsulated, free-floating islets. In all cases, free-floating islets respond well to glucose challenge. The islets encapsulated within the commercial large diameter (PESM) fibers function neither after 1 d nor after 7 d of culture (stimulation index for high glucose concentration below 2, see Figure 5A). In contrast, islets encapsulated within the new multibore (MF3-washed) fibers respond to changing glucose concentrations and retain their endocrine function during the 7 d culture period indicating also their viability after encapsulation within the bores of the novel fiber (Figure 5B).

We also studied the potential of the multibore fibers to encapsulate graded loads of human islets from one donor. We performed various experiments where in total of 1000, 3000, or 6000 islets per cm fiber were encapsulated to determine whether higher loads may impair the glucose-induced insulin response.

Figure 5C compares the amount of insulin secreted from the islets encapsulated in the MF3 washed membranes to free-floating islets after 7 d of culture. In all cases, the free-floating islets (Figure 5C and zoom on Figure 5D), as well as the islets encapsulated within the fibers function well showing a clear response to glucose concentration changes during all five glucose incubation steps. In fact, the amount of secreted insulin increases with the number of islets encapsulated in the membrane indicating that islet viability was also maintained. Statistical analysis showed a significant difference in insulin secretion between the various number of islets used for encapsulation ( $p < 0.05$ ). Basal insulin concentration after first low

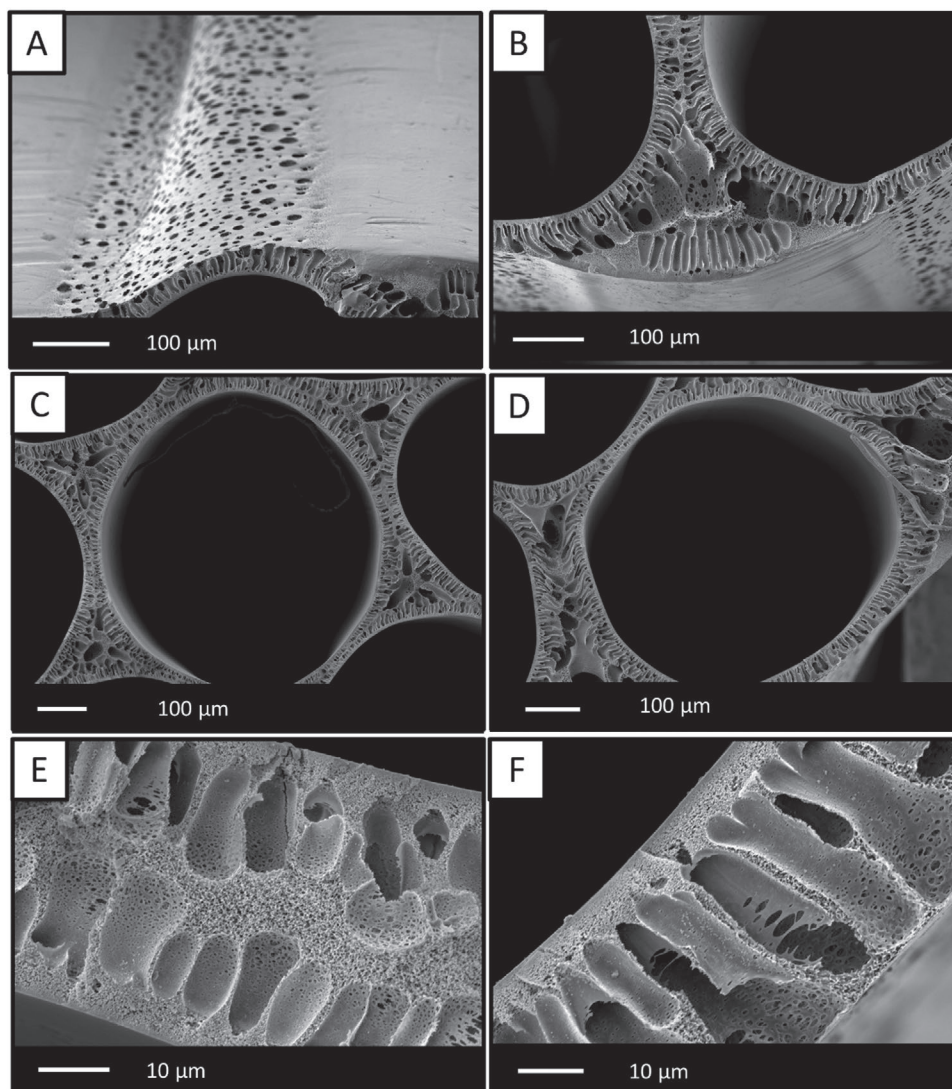


**Figure 3.** Scanning electron microscopy images of multibore hollow fiber—MF3: A) outer bore surface, B) cross section of outer connection between two bores, C) middle bore cross section, D) side bore cross section, E) cross section of the wall between two bores, and F) cross section of the bore outer wall.

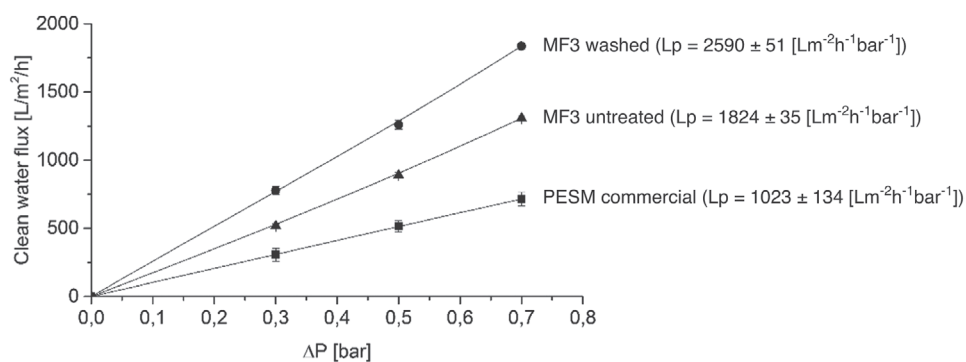


**Figure 4.** Clean water flux versus transmembrane pressure for commercial PESM membranes, MF3-untreated new multibore hollow fiber and MF3 washed with NaClO for 24 h. Error bars indicate standard deviation ( $n = 3$ ).

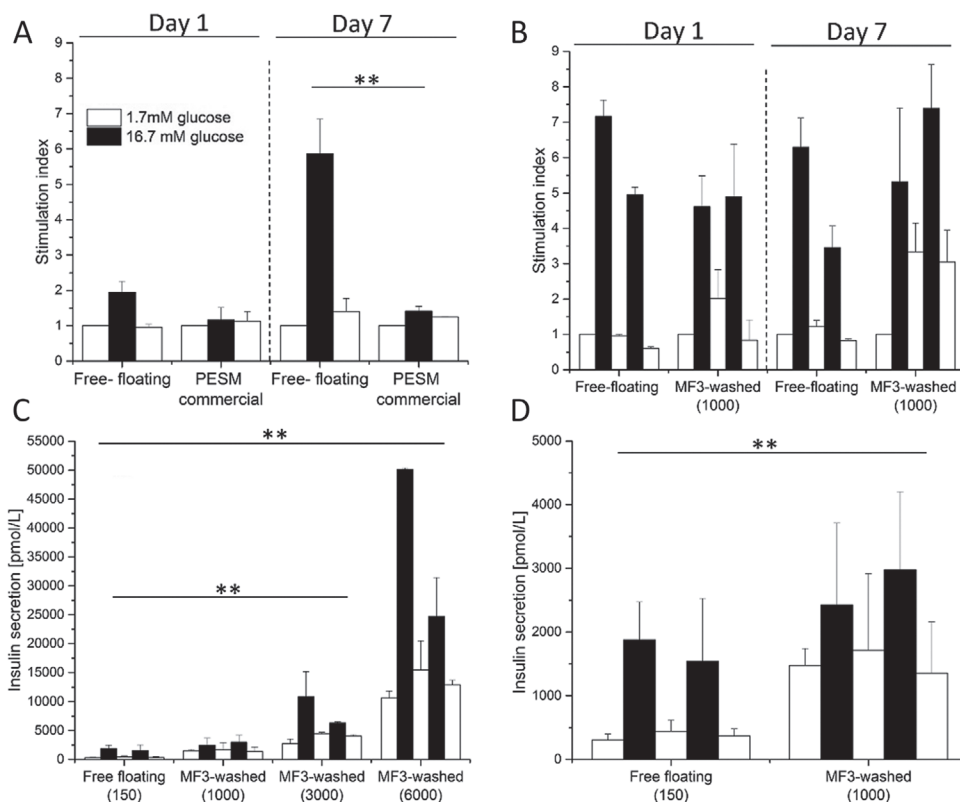


**Figure 5.** Functionality test of encapsulated islets: A) stimulation index after day 1 and 7 for islets encapsulated within commercial PESM membranes (1 cm fiber, 3500 islets; 150 free floating islets) (the graph reproduced with permission from ref. [17]), B) stimulation index after day 1 and 7 of encapsulated islets from donor 1 within MF3-washed (1000 islets,  $n = 3$ ), C) insulin secretion of different number of human islets from donor 2 after 7 d of culture, encapsulated within MF3-washed, D) zoomed-in insulin secretion of free floating islets and 1000 islets encapsulated within MF3-washed. Error bars indicate standard deviation ( $n = 3$ ),  $**p < 0.05$ .

glucose stimulation was  $1500 \text{ pmol L}^{-1}$  for 1000 islets and almost double ( $2741 \text{ pmol L}^{-1}$ ) when 3000 islets/fiber were encapsulated, reaching  $10657 \text{ pmol L}^{-1}$  for 6000 islets/fiber. Furthermore, upon the first high glucose stimulation, the insulin concentration for 6000 encapsulated islets/fiber is more than double than for 3000 islets/fiber and about 20 times higher than for 1000 encapsulated islets/fiber. The following glucose concentration changes resulted in an adequate response, namely, a decrease in insulin secretion for low glucose concentration and an increase of insulin secretion for high glucose concentration, not statistically different from free-floating islets ( $p > 0.05$ ), indicating that islets remain functional within the multibore fibers.

**Figure 6** shows the stimulation index of islets from two other donors, encapsulated within the new multibore fibers, compared to the free-floating islets. The islets from both donors secrete insulin upon glucose stimulation after 1 d of culture and they retain their endocrine function after 7 d of culture, similar to free-floating nonencapsulated islets (no statistical difference:  $p > 0.05$ ). In all cases, the stimulation index of the first high glucose stimulation is more than double compared to basal insulin release. Again, even when a high number of islets is used, the encapsulation device remains functional for cells of all used donors. Since there is a significant variation between donors ( $p < 0.05$ ), we also found that the free-floating islets from donor 3 secreted higher amount of insulin (Figure S2,

Supporting Information) and showed higher response to glucose concentration changes (Figure 6A) in comparison to less responsive islets from donor 4, where stimulation index was less than 3 for high glucose stimulation (Figure 6B,C). The insulin secretion was also higher for the islets from donor 3. Importantly, we also observe an increase in stimulation index after the second and third low glucose stimulation for all number of encapsulated islets within the fibers in comparison to basal insulin release although the difference is not significant ( $p > 0.05$ ). Perhaps, insulin produced during the previous high glucose incubation step is slowly released during the next low glucose stimulation steps. Another reason for this could be that the glucose was not completely removed from the device after high glucose incubation and, therefore, the final concentration used for the next incubation step was higher than  $1.7 \times 10^{-3} \text{ M}$ , causing an increased islet response. Despite this, for all number of encapsulated islets we observe a clear response to the first increase of glucose concentration over 7 d of culture.

### 3.4. Fiber Material Biocompatibility and Blood Vessel Formation: Preliminary In Vivo Study

In order to assess the biocompatibility of multibore fiber material, fibers (1 cm) were implanted subcutaneously in mice. Animal behavior after implantation was normal, with



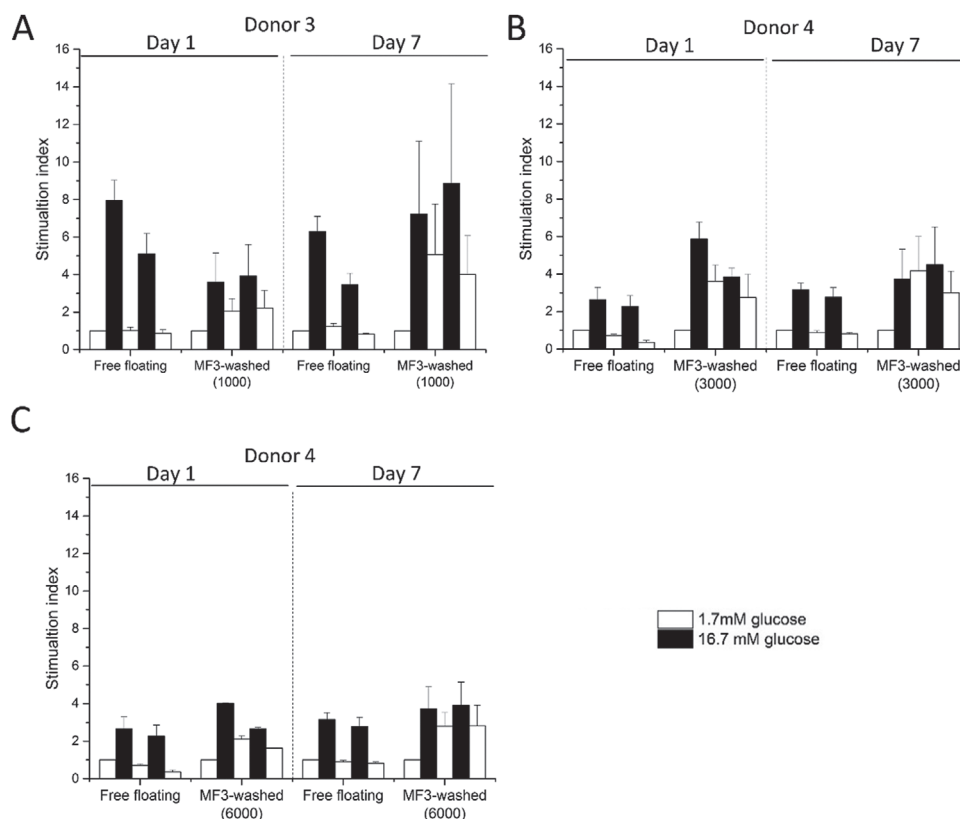


**Figure 6.** Human islets functionality within new multibore hollow fiber membranes (MF3-washed) in comparison to free floating islets (150) after 1 and 7 d of culture: A) encapsulated 1000 islets from donor 3, B) encapsulated 3000 islets from donor 4, and C) encapsulated 6000 islets from donor 4. Error bars indicate standard deviation ( $n = 3$ ).

an increase in their weight over the study period (see Figure S3, Supporting Information). After 28 d the animals were sacrificed, and fibers were, after macroscopical examination in the implantation site, carefully removed for histological analysis. Macroscopically, we did not observe inflammation in the implantation site. Moreover, the device was not integrated in the surrounding tissue, illustrating optimal biocompatibility of

the device material. **Figure 7A** shows a cross section of the fiber with a thin layer of surrounding tissue (50–250  $\mu\text{m}$ ) mainly composed of cells with the morphological characteristics of fibroblasts. Importantly, the device was surrounded by blood filled capillaries (Figure S3, Supporting Information). Although the vascularization was minor, we did in fact observe blood vessels close (less than 50  $\mu\text{m}$ ) to the fiber (Figure 7B). To confirm

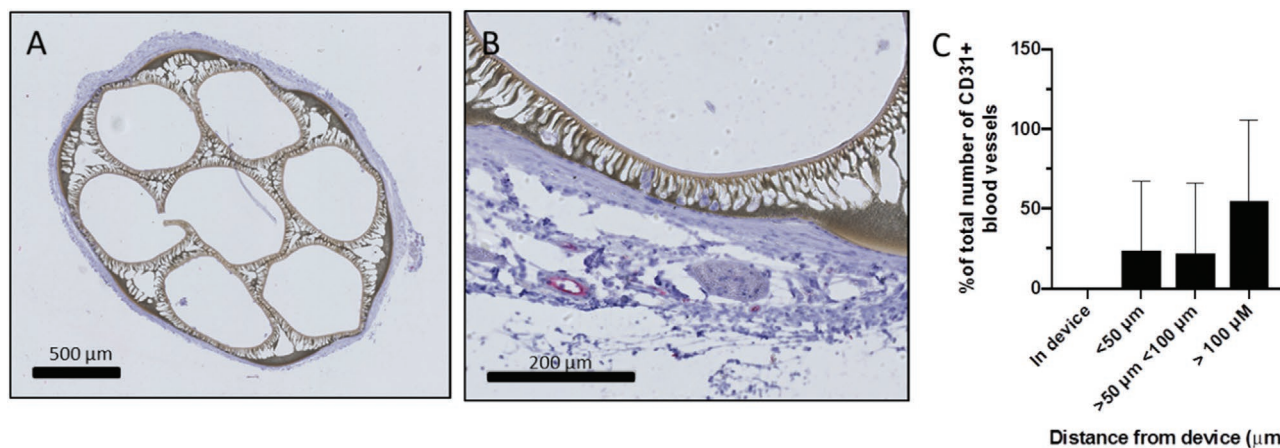


**Figure 7.** Multibore fiber implantation study: A) HE stained section of the fiber after 28 d of implantation, B) representative fiber section with a few CD31 positive (red) endothelial cells, and C) percentage of CD31 positive blood vessels and their distance from the device after 28 d of implantation. Error bars indicate standard deviation ( $n = 5$ ).

blood vessel formation immunocytochemically, sections were additionally stained for CD31 positive cells. There was no statistical difference in the number of CD31 positive cells found in less than 50  $\mu\text{m}$ , between 50 and 100  $\mu\text{m}$  or above 100  $\mu\text{m}$  distance from the device (Figure 7C). It seems that although the pore size on the outside of the fibers was designed to be low to avoid cell infiltration, some cells were able to infiltrate to the thin fiber walls on the outside of the fiber. However, endothelial cells were only observed there and could not penetrate to the lumen of the fiber where the islets would be encapsulated.

#### 4. Discussion

One of the advantages of hollow fibers over flat membranes for macroencapsulation of islet grafts is their large surface area to volume ratio which is desirable in order to encapsulate a high number of islets in a relatively small volume.<sup>[18]</sup> However, single fibers applied as macroencapsulation devices often have low mechanical stability. They tend to bend and break, which consequently could lead to islet loss after transplantation.<sup>[19]</sup> In this study, we propose a new islet macroencapsulation device based on porous multibore fiber membranes. They consist of seven equally spaced bores, where the bore diameter is optimized to host a range of sizes of human islets. The membrane structure provides one of the best geometries for hollow fiber membranes and ensures both large porosity and excellent mechanical properties.<sup>[13]</sup> High stability is a great advantage of the multibore membranes, important for handling process and for resisting mechanical forces in the period before, during, and after transplantation.

In order to provide long-term islet encapsulation, the fibers were fabricated using nondegradable PES/PVP polymer blend. PES is a widely used biomaterial for hemodialysis membranes, with excellent chemical and mechanical properties.<sup>[14]</sup> The PVP improves material biocompatibility and introduces non-cell-adhesive properties to avoid cell attachment onto the membrane surface, which is important for islet transplantation.<sup>[20]</sup> In the literature, other materials have been proposed for hollow fiber fabrication, such as modified polyacrylonitrile polyvinyl chloride,<sup>[21]</sup> regenerated cellulose and polyamide,<sup>[8b]</sup> acrylic copolymer (XM-50 Amicon),<sup>[22]</sup> and polysulfone.<sup>[23]</sup> However, the need to use large numbers of islets encapsulated in hollow fibers with relatively big diameter (0.6–3 mm)<sup>[24]</sup> led to limited transport of nutrients and oxygen, and consequently islet death.

The new multibore hollow fibers were fabricated using dry-wet spinning method via immersion precipitation.<sup>[25]</sup> By changing the spinning parameters: composition of bore liquid and coagulation bath temperature, we obtained highly porous membranes with bores of 500  $\mu\text{m}$  and very thin walls ( $\approx 40$   $\mu\text{m}$ ). This was achieved by adding solvent (NMP) in the bore liquid which reduced the rate of phase separation; the exchange between solvent and nonsolvent (lower concentration gradients during solvent/nonsolvent exchange). As a result, we obtained a relatively spongy membrane structure with small voids and high porosity (MF2). The fiber wall thickness was decreased, and the pore morphology was improved in comparison to MF1 membranes (Figure 2B). When pure

nonsolvent (water) was used as a bore liquid, the formation of dense inner surface occurred. The addition of NMP in the bore solution can increase the porosity of the inner surface and can prevent the formation of a dense skin layer.<sup>[26]</sup> However, the exchange of solvent and nonsolvent on the inner surface of our fiber lumen was slower than on the outside surface of the fiber, resulting in deformation of the bores. Mousavi et al. studied the effects of various temperatures of the coagulation bath on the formation of polyethersulfone membranes and found out that increase in the temperature of the coagulation bath leads to an increase in the solvent–nonsolvent exchange rate.<sup>[27]</sup> Subsequently, a more porous structure is formed resulting in higher membrane permeability.<sup>[28]</sup> When we increased the coagulation bath temperature, we obtained MF3 membranes with improved outer surface porosity. The combination of tailoring the bore liquid composition and the temperature of coagulation bath resulted in a proper exchange rate during the phase separation process, resulting in stable and highly porous multibore fibers with desired bore dimensions and thin walls. The latter is a very important requirement for optimal mass transport during islet encapsulation, since the cell survival depends on the diffusion distance of nutrients to the cells. When this exceeds 200  $\mu\text{m}$ , it is known that cell survival can be negatively affected.<sup>[4b]</sup>

Multibore hollow fiber membranes are presented in literature for various applications. Wang and Chung designed and fabricated a lotus-root multibore hollow fiber membrane for membrane distillation process.<sup>[13]</sup> This concept has also been adopted for inorganic ceramic membranes.<sup>[29]</sup> In recent years, a seven-bore ultrafiltration hollow fiber membrane has been fabricated using a specially modified polyethersulfone material (PESM) by Inge GmbH. Here, we compared these membranes to our new developed multibore fibers for islet encapsulation. Our optimal hollow fiber (MF3 washed) is two times smaller than these commercial PESM membranes considering both outer membrane and bore diameter. Besides our fibers have high permeability (2590 L m<sup>-2</sup> h<sup>-1</sup> bar<sup>-1</sup>), more than double in comparison to the permeability of commercial membranes and others with similar pore size (0.05–5  $\mu\text{m}$ ).<sup>[15]</sup>

The tailor-made MF3 membranes were used for encapsulating pancreatic islets and were compared to commercial PESM membranes and to nonencapsulated (free-floating) islets. De Bartolo et al. had shown earlier that highly permeable PESM membranes allow for transport of bovine serum albumin (66.5 kDa), which is a much bigger molecule than insulin or glucose.<sup>[15b]</sup> However, human islets encapsulated within PESM membranes did not respond to glucose concentration changes, which could be attributed to suboptimal dimensions of the fiber. The large bore diameter (0.9 mm) and the thick walls of the fiber, probably limit the diffusion of nutrients to cells, which negatively affects islet survival and function. In contrast, our multibore hollow fibers, especially designed for this application, succeeded and the encapsulated islets remained functional over 7 d of culture.

Single bore fibers have been used for the encapsulation of a low number of islets. Lambert et al. encapsulated 50 islets within 1 cm hydroxyl-methylated polysulfone fiber (0.9 mm inner diameter).<sup>[23]</sup> Here, we used all available volume of the

fiber and we were able to encapsulate up to 6000 islets inside a 1 cm long fiber without impairing survival in culture up to 7 d. We observed that the concentration of secreted insulin increases with the number of encapsulated islets, indicating that the membrane porosity is sufficient to provide nutrients to the cells and achieve good insulin delivery by the cells. We showed that the human islets encapsulated within the bores of our fiber secrete insulin in response to glucose concentration changes and function well after 7 d of culture, despite the variability in the quality of human islets obtained from various donors.

The material used for the fiber fabrication was proven to be biocompatible in our implantation study. After 28 d we did not observe significant adhesion of inflammatory cells. This is an important observation as most deleterious cytokines are smaller than, e.g., insulin and can pass the membrane.<sup>[30]</sup> Cells on the surface of the device can also compete for nutrients and thereby influence function of cells inside the device.<sup>[31]</sup> The thickness of the surrounding fibroblast layer was similar to poly(D,L-lactide-co-epsilon-caprolactone) based devices but less than what we have observed on polysulfone and polyactive-based formulation.<sup>[32]</sup> Except for this, there is ongoing debate about the need for adequate amounts of blood vessels as close as possible to the membranes for fast exchange of glucose and insulin as well as of nutrients.<sup>[4c]</sup> To the best of our knowledge we are the first to show that vessels can grow in as close as 50 μm from the hollow fiber membrane surface.<sup>[4c]</sup> The vessel density we observed with the current device was similar to what we have observed with other devices we have tested and the beta-O2 device that have demonstrated adequate exchange of glucose and insulin and therewith regulation of blood glucose.<sup>[33]</sup>

In encapsulation studies, separation factors such as particles and/or gels are used to avoid islets aggregation. Here, we avoided the use of separation factors during islet seeding to prevent additional diffusion transport barriers.<sup>[34]</sup> Perhaps, the lack of separation factors creates empty space between the membrane walls and the encapsulated islets, where secreted insulin or glucose could be trapped and then is slowly released. Although, the islets were freely distributed in the fiber and did not attach to the membrane surface due to low-adhesive material properties (see Figure S4, Supporting Information), the histological analysis remained challenging due to islet loss during sample cutting and processing and a comparison between the various number of islets encapsulated within the MF3 membranes could not be performed. As the cells could not attach to the membrane surface, the viability of the islets encapsulated within the fibers was not assessed due to possible loss of islets after opening the bores of the fiber. Nevertheless, the insulin response to glucose concentration changes is clear indicating the potential of the application of these multibore hollow fibers for islet macroencapsulation.

Finally, our preliminary implantation study shows the fiber material biocompatibility with minimal tissue response toward fiber material, indicating a promising application of new multibore fibers for islet encapsulation in vivo. Moreover, we observed the formation of blood vessels within 200 μm distance from the implanted device, which is important considering high islet metabolic activity and their need for proximity to the source of oxygen and nutrients.<sup>[4c]</sup>

## 5. Conclusion and Outlook

In this study, we have developed new PES/PVP multibore hollow fiber membrane for islet macroencapsulation. The membranes are nondegradable, mechanically stable and allow the encapsulation of a high number of islets, crucial for device upscaling and clinical application. The optimized bore dimensions and membrane porosity provide sufficient glucose and insulin transport, important for maintaining islet function. Moreover, material biocompatibility supports the formation of blood vessels close to the multibore fiber which is crucial for encapsulated islet survival in vivo.

Following the promising in vitro results obtained here, future studies would focus on the application of the multibore hollow fibers as islet macroencapsulation devices and assessment of cell survival and functionality in vivo, using firstly small animal models and later possibly in humans. For these studies, the size of the device necessary to accommodate a sufficient number of islets is very important. To be able to compare the volume of islets with different diameters and volumes, individual islets are mathematically converted to standard islet equivalents (IEQs) with a diameter of 150 μm.<sup>[35]</sup> It has been estimated that 9000 IEQs per kilo bodyweight of patient are needed to restore normoglycaemia.<sup>[1b]</sup> Therefore, by using multibore fibers with cells encapsulated within the six equally spaced bores, leaving the middle bore for possible vascularization or better nutrient supply, we would need eight multibore hollow fibers of 20 cm (11250 IEQs per bore, 50% fiber loading capacity) in order to treat a 60 kg patient. The seeding method applied in this study allows for the connection of a longer fiber to the syringe which should contain the islet number adapted to the volume of the available bores. To minimize the space needed for implantation, the fibers could be coiled (in a ring of about 6 cm in diameter) without affecting membrane properties due to their high mechanical stability in comparison to single bore fibers. Islet encapsulation within semipermeable membranes might have additionally potential to provide adequate immune-isolation and allow for transplantation in the absence of immunosuppression. Therefore, the immunoprotective properties of our multibore fibers will be investigated in the future.

## Supporting Information

Supporting Information is available from the Wiley Online Library or from the author.

## Acknowledgements

This research was financially supported by i) the Juvenile Diabetes Research Foundation; grant title: New islet encapsulation method for ideal mass transport and immune protection; grant key: 17-2013-303 and ii) the Dutch NWA Impulse project: Spearheads for the quantum and nano revolution, Dossier No. 400.17.607.

## Conflict of Interest

The authors declare no conflict of interest.

## Author Contributions

K.S. performed literature search, experimental design, data collection, data analysis, and manuscript writing. M.G.N. and J.L.-V. contributed to experimental design, data collection, analysis, and manuscript writing. A.M.S. and E.S. contributed to data collection, analysis, and manuscript writing. M.A.E. and E.J.P.d.K. provided human islets for experiments and performed manuscript writing. M.K. and P.d.V. contributed to the results discussion and to the manuscript writing. A.v.A., P.d.V., and D.S. contributed to experimental design, data interpretation, and manuscript writing.

## Keywords

hollow fibers, islet, macroencapsulation, membranes, multibore, pancreas

Received: January 16, 2020

Revised: June 2, 2020

Published online:

- [1] a) A. M. J. Shapiro, C. Ricordi, B. J. Hering, H. Auchincloss, R. Lindblad, R. P. Robertson, A. Secchi, M. D. Brendel, T. Berney, D. C. Brennan, E. Cagliero, R. Alejandro, E. A. Ryan, B. DiMercurio, P. Morel, K. S. Polonsky, J.-A. Reems, R. G. Bretzel, F. Bertuzzi, T. Froud, R. Kandaswamy, D. E. R. Sutherland, G. Eisenbarth, M. Segal, J. Preiksaitis, G. S. Korbutt, F. B. Barton, L. Viviano, V. Seyfert-Margolis, J. Bluestone, J. R. T. Lakey, *N. Engl. J. Med.* **2006**, 355, 1318; b) E. A. Ryan, J. R. Lakey, R. V. Rajotte, G. S. Korbutt, T. Kin, S. Imes, A. Rabinovitch, J. F. Elliott, D. Bigam, N. M. Kneteman, G. L. Warnock, I. Larsen, A. M. Shapiro, *Diabetes* **2001**, 50, 710.
- [2] a) P.-O. Carlsson, *Upsala J. Med. Sci.* **2011**, 116, 1; b) O. Korsgren, T. Lundgren, M. Felldin, A. Foss, B. Isaksson, J. Permert, N. H. Persson, E. Rafael, M. Ryden, K. Salmela, A. Tibell, G. Tufveson, B. Nilsson, *Diabetologia* **2008**, 51, 227.
- [3] a) S. Merani, C. Toso, J. Emamaullee, A. M. Shapiro, *Br. J. Surg.* **2008**, 95, 1449; b) R. F. Gibly, X. Zhang, M. L. Graham, B. J. Hering, D. B. Kaufman, W. L. Lowe, L. D. Shea, *Biomaterials* **2011**, 32, 9677; c) R. F. Gibly, X. Zhang, W. L. Lowe, L. D. Shea, *Cell Transplant.* **2013**, 22, 811.
- [4] a) V. Iacovacci, L. Ricotti, A. Menciasci, P. Dario, *Biochem. Pharmacol.* **2016**, 100, 12; b) J. Schweicher, C. Nyitray, T. A. Desai, *Front. Biosci.* **2014**, 19, 49; c) U. Barkai, A. Rotem, P. de Vos, *World J. Transplant.* **2016**, 6, 69.
- [5] P. de Vos, A. F. Hamel, K. Tatarikiewicz, *Diabetologia* **2002**, 45, 159.
- [6] S. Hu, P. de Vos, *Front. Bioeng. Biotechnol.* **2019**, 7, 134.
- [7] H. K. Tilakaratne, S. K. Hunter, M. E. Andracki, J. A. Benda, V. G. J. Rodgers, *Biomaterials* **2007**, 28, 89.
- [8] a) J. J. Altman, *J. Diabetic Complications* **1988**, 2, 68; b) T. Zekorn, U. Siebers, L. Filip, K. Mauer, U. Schmitt, R. G. Bretzel, K. Federlin, *Transplant. Proc.* **1989**, 21, 2748.
- [9] a) A. Andersson, *Diabetologia* **1978**, 14, 397; b) M. Buitinga, R. Truckenmüller, M. A. Engelse, L. Moroni, H. W. M. Ten Hoopen, C. A. van Blitterswijk, E. J. P. de Koning, A. A. van Apeldoorn, M. Karperien, *PLoS One* **2013**, 8, e64772.
- [10] a) T. Maki, C. J. Mullon, B. A. Solomon, A. P. Monaco, *Clin. Pharmacokinet.* **1995**, 28, 471; b) T. Maki, C. S. Ubhi, H. Sanchez-Farpon, S. J. Sullivan, K. Borland, T. E. Muller, B. A. Solomon, W. L. Chick, A. P. Monaco, *Transplantation* **1991**, 51, 43; c) A. I. Silva, A. N. de Matos, I. G. Brons, M. Mateus, *Med. Res. Rev.* **2006**, 26, 181.
- [11] J. L. Dulong, C. Legallais, *J. Biomech. Eng.* **2005**, 127, 1054.
- [12] J. L. Dulong, C. Legallais, *Biotechnol. Bioeng.* **2007**, 96, 990.
- [13] P. Wang, T.-S. Chung, *J. Membr. Sci.* **2012**, 421, 361.
- [14] M. Irfan, A. Idris, *Mater. Sci. Eng., C* **2015**, 56, 574.
- [15] a) N. M. S. Bettahalli, *Ph.D. Thesis, University of Twente, Enschede* **2011**; b) L. De Bartolo, S. Morelli, M. Rende, C. Campana, S. Salerno, N. Quintiero, E. Drioli, *Macromol. Biosci.* **2007**, 7, 671.
- [16] N. Lambert, J. Wesche, P. Petersen, P. Zschocke, A. Enderle, H. Planck, H. P. Ammon, *Exp. Clin. Endocrinol. Diabetes* **2001**, 109, 116.
- [17] M. Groot Nibbelink, *Ph.D. Thesis, University of Twente, Enschede* **2016**.
- [18] G. Meneghello, D. J. Parker, B. J. Ainsworth, S. P. Perera, J. B. Chaudhuri, M. J. Ellis, P. A. De Bank, *J. Membr. Sci.* **2009**, 344, 55.
- [19] N. Sakata, S. Sumi, G. Yoshimatsu, M. Goto, S. Egawa, M. Unno, *World J. Gastrointest. Pathophysiol.* **2012**, 3, 19.
- [20] a) H. Wang, T. Yu, C. Zhao, Q. Du, *Fibers Polym.* **2009**, 10, 1; b) F. Ran, S. Nie, W. Zhao, J. Li, B. Su, S. Sun, C. Zhao, *Acta Biomater.* **2011**, 7, 3370.
- [21] D. W. Scharp, C. J. Swanson, B. J. Olack, P. P. Latta, O. D. Hegre, E. J. Doherty, F. T. Gentile, K. S. Flavin, M. F. Ansara, P. E. Lacy, *Diabetes* **1994**, 43, 1167.
- [22] A. M. Sun, W. Parisius, G. M. Healy, I. Vacek, H. G. Macmorine, *Diabetes* **1977**, 26, 1136.
- [23] N. Lambert, P. Petersen, J. Wesche, P. Zschocke, A. Enderle, M. Doser, H. Planck, H. D. Becker, H. P. Ammon, *Ann. N. Y. Acad. Sci.* **2001**, 944, 271.
- [24] a) A. V. Prochorov, S. I. Tretjak, V. A. Goranov, A. A. Glinnik, M. V. Goltsev, *Adv. Med. Sci.* **2008**, 53, 240; b) P. E. Lacy, O. D. Hegre, A. Gerasimidi-Vazeou, F. T. Gentile, K. E. Dionne, *Science* **1991**, 254, 1782; c) N. Lambert, J. Wesche, P. Petersen, M. Doser, P. Zschocke, H. D. Becker, H. P. T. Ammon, *Cell Transplant.* **2005**, 14, 97.
- [25] I. M. Wien, F. H. A. Olde scholtenhuis, T. v. d. Boomgaard, C. A. Smolders, *J. Membr. Sci.* **1995**, 106, 233.
- [26] a) M. Rahbari-sisakht, A. F. Ismail, T. Matsuura, *Sep. Purif. Technol.* **2012**, 88, 99; b) C. C. Pereira, R. Nobrega, C. P. Borges, *Braz. J. Chem. Eng.* **2000**, 17, 599.
- [27] S. M. Mousavi, F. Dehghan, E. Saljoughi, S. A. Hosseini, *J. Polym. Res.* **2012**, 19, 9861.
- [28] R. Sengur-Tasdemir, G. M. Urper, T. Turken, E. A. Genceli, V. V. Tarabara, I. Koyuncu, *Sep. Sci. Technol.* **2016**, 51, 2070.
- [29] a) Y. Zhang, C. Qin, J. Binner, *Ceram. Int.* **2006**, 32, 811; b) A. F. Ismail, K. Li, *Membrane Science and Technology*, Vol. 13, Elsevier, Amsterdam **2008**, p. 81.
- [30] P. de Vos, I. Smedema, H. van Goor, H. Moes, J. van Zanten, S. Netters, L. F. de Leij, A. de Haan, B. J. de Haan, *Diabetologia* **2003**, 46, 666.
- [31] P. de Vos, G. H. Wolters, R. van Schilfgaarde, *Transplant. Proc.* **1994**, 26, 782.
- [32] a) A. M. Smink, B. J. de Haan, G. A. Paredes-Juarez, A. H. Wolters, J. Kuipers, B. N. Giepmans, L. Schwab, M. A. Engelse, A. A. van Apeldoorn, E. de Koning, M. M. Faas, P. de Vos, *Biomed. Mater.* **2016**, 11, 035006; b) A. M. Smink, D. T. Hertsig, L. Schwab, A. A. van Apeldoorn, E. de Koning, M. M. Faas, B. J. de Haan, P. de Vos, *Ann. Surg.* **2017**, 266, 149; c) A. M. Smink, S. Li, D. T. Hertsig, B. J. de Haan, L. Schwab, A. A. van Apeldoorn, E. de Koning, M. M. Faas, J. R. Lakey, P. de Vos, *Transplantation* **2017**, 101, e112.
- [33] a) U. Barkai, G. C. Weir, C. K. Colton, B. Ludwig, S. R. Bornstein, M. D. Brendel, T. Neufeld, C. Bremer, A. Leon, Y. Evron, K. Yavriyants, D. Azarov, B. Zimmermann, S. Maimon, N. Shabtay, M. Balyura, T. Rozenshtein, P. Vardi, K. Bloch, P. de Vos, A. Rotem, *Cell Transplant.* **2013**, 22, 1463; b) Y. Evron, C. K. Colton, B. Ludwig, G. C. Weir, B. Zimmermann, S. Maimon, T. Neufeld, N. Shalev,





- T. Goldman, A. Leon, K. Yavriyants, N. Shabtay, T. Rozenshtein, D. Azarov, A. R. Dilenno, A. Steffen, P. de Vos, S. R. Bornstein, U. Barkai, A. Rotem, *Sci. Rep.* **2018**, *8*, 6508; c) T. Neufeld, B. Ludwig, U. Barkai, G. C. Weir, C. K. Colton, Y. Evron, M. Balyura, K. Yavriyants, B. Zimmermann, D. Azarov, S. Maimon, N. Shabtay, T. Rozenshtein, D. Lorber, A. Steffen, U. Willenz, K. Bloch, P. Vardi, R. Taube, P. de Vos, E. C. Lewis, S. R. Bornstein, A. Rotem, *PLoS One* **2013**, *8*, e70150.
- [34] a) J.-J. Qin, M. H. Oo, Y. Li, *J. Membr. Sci.* **2005**, *247*, 137; b) S. Rouaix, C. Causserand, P. Aimar, *J. Membr. Sci.* **2006**, *277*, 137.
- [35] C. Ricordi, D. W. R. Gray, B. J. Hering, D. B. Kaufman, G. L. Warnock, N. M. Kneteman, S. P. Lake, N. J. M. London, C. Socci, R. Alejandro, Y. Zeng, D. W. Scharp, G. Viviani, L. Falqui, A. Tzakis, R. G. Bretzel, K. Federlin, G. Pozza, R. F. L. James, R. V. Rajotte, V. D. Carlo, P. J. Morris, D. E. R. Sutherland, T. E. Starzl, D. H. Mintz, P. E. Lacy, *Acta Diabetol. Lat.* **1990**, *27*, 185.